

# Effect of photon energy spectrum on dosimetric parameters of brachytherapy sources

Mahdi Ghorbani<sup>1</sup>, Mohammad Mehrpouyan<sup>2</sup>, David Davenport<sup>3</sup>, Toktam Ahmadi Moghaddas<sup>4</sup>

<sup>1</sup> Medical Physics Research Center, Mashhad University of Medical Sciences, Mashhad, Iran

<sup>2</sup> Bioinformatics Research Center, Sabzevar University of Medical Sciences, Sabzevar, Iran

<sup>3</sup> Comprehensive Cancer Centers of Nevada, Las Vegas, Nevada, USA

<sup>4</sup> Department of Basic Medical Sciences, Neyshabur University of Medical Sciences, Neyshabur, Iran

Radiol Oncol 2016; 50(2): 238-246.

Received 2 November 2015

Accepted 29 January 2016

Correspondence to: Mohammad Mehrpouyan, Bioinformatics Research Center, Sabzevar University of Medical Sciences, Sabzevar, Iran. Phone: +98 51 4444 6070, +98 51 4444 6234; Fax: +98 51 4444 5648; E-mail: mehrpouyan.mohammad@gmail.com; or Toktam Ahmadi Moghaddas, Department of Basic Medical Sciences, Neyshabur University of Medical Sciences, Neyshabur, Iran. E-mail: toktamt.moghaddas@gmail.com

Disclosure: No potential conflicts of interest were disclosed.

**Aim.** The aim of this study is to quantify the influence of the photon energy spectrum of brachytherapy sources on task group No. 43 (TG-43) dosimetric parameters.

**Background.** Different photon spectra are used for a specific radionuclide in Monte Carlo simulations of brachytherapy sources.

**Materials and methods.** MCNPX code was used to simulate <sup>125</sup>I, <sup>103</sup>Pd, <sup>169</sup>Yb, and <sup>192</sup>Ir brachytherapy sources. Air kerma strength per activity, dose rate constant, radial dose function, and two dimensional (2D) anisotropy functions were calculated and isodose curves were plotted for three different photon energy spectra. The references for photon energy spectra were: published papers, Lawrence Berkeley National Laboratory (LBNL), and National Nuclear Data Center (NNDC). The data calculated by these photon energy spectra were compared.

**Results.** Dose rate constant values showed a maximum difference of 24.07% for <sup>103</sup>Pd source with different photon energy spectra. Radial dose function values based on different spectra were relatively the same. 2D anisotropy function values showed minor differences in most of distances and angles. There was not any detectable difference between the isodose contours.

**Conclusions.** Dosimetric parameters obtained with different photon spectra were relatively the same, however it is suggested that more accurate and updated photon energy spectra be used in Monte Carlo simulations. This would allow for calculation of reliable dosimetric data for source modeling and calculation in brachytherapy treatment planning systems.

Key words: photon energy spectrum; brachytherapy; TG-43 dosimetric parameters; dose distribution

## Introduction

Monte Carlo (MC) codes are currently used to verify brachytherapy sources while utilizing the photon energy spectrum of a specific radionuclide for calculations. There exist some common energy spectrum databases which are used by researchers. Some use the recommendation of the American

Association of Physicists in Medicine (AAPM) from task group No. 43 updated report (TG-43 U1) which was prepared for low energy photon emitting radionuclides such as <sup>125</sup>I and <sup>103</sup>Pd.<sup>1</sup> In a report by the AAPM and the European Society for Therapeutic Radiology and Oncology (ESTRO)<sup>2</sup>, the use of the energy spectrum database of the National Nuclear Data Center (NNDC)<sup>3</sup> was rec-

ommended for photon emitting radionuclides higher than 50 keV.

There are various methods to determine the energy spectra of photon emitting radionuclides. One widely used technique is high-purity germanium detectors, especially for low energy sources.<sup>4-6</sup> Chen *et al.*<sup>7</sup>, have used a high purity germanium detector to measure the photon energy spectrum emitted by a <sup>125</sup>I brachytherapy source. Rivard *et al.*<sup>8</sup> have studied the influence of photon energy spectrum on kerma and dose rate for <sup>125</sup>I, <sup>103</sup>Pd, and <sup>192</sup>Ir sources. They calculated the water kerma proportion for each photon energy to the total energy and plotted the obtained data for different distances. It was concluded that the differences in photon energy spectra do not have a considerable impact on the dose rate constant because of the compensatory effect of dividing dose rate to air kerma strength. In a study by Aryal *et al.*<sup>9</sup>, TG-43 dosimetry parameters were calculated for IAI <sup>125</sup>I brachytherapy source by variation of some factors such as photon energy spectrum. They found that the photon energy spectrum can change dose rate constant by up to 3% and can alter radial dose function about 12% (at  $r = 10$  cm where the dose rate is very low).

It is necessary to implement TG-43 dosimetric parameters in treatment planning systems.<sup>10</sup> <sup>125</sup>I brachytherapy source models are widely used in prostate cancer treatments wherein the dose received by organs at risk such as rectum and urinary bladder is important. To quantify the dose to these organs, treatment planning systems use the appropriate TG-43 dosimetric parameters which were reported in the literature. Treatment planning systems do not use energy spectrum directly, but they use TG-43 parameters reported by a published study. Therefore, the energy spectrum used in that study can effect on the calculation accuracy of the treatment planning systems indirectly. So the precision of energy spectrum of the radionuclide can have influences on the calculated dose to the tumor and the related organs at risk. Therefore, it is important to provide accurate energy spectra of radionuclides. In the previously mentioned studies, only some dosimetric parameters were evaluated from the energy spectrum point of view. To the best of our knowledge, a comprehensive study considering the influence of photon energy spectrum on the dosimetric parameters of brachytherapy sources was not performed.

The aim of this study is to evaluate the influence of photon energy spectrum on TG-43 dosimetric parameters and isodose curves for three common

photon energy spectra; for <sup>125</sup>I, <sup>103</sup>Pd, <sup>169</sup>Yb, and <sup>192</sup>Ir brachytherapy sources.

## Materials and methods

In this study, MCNPX code (version 2.4.0) was used to simulate brachytherapy sources.<sup>11</sup> Four brachytherapy sources were studied: MED 3631-A/M <sup>125</sup>I, Optiseed <sup>103</sup>Pd, a hypothetical <sup>169</sup>Yb, and Flexisource <sup>192</sup>Ir sources. In the selection of these radionuclides, there was an attempt to evaluate various brachytherapy sources within a relatively wide range of photon energies. The MED 3631-A/M <sup>125</sup>I source consists of four polystyrene spheres coated with active <sup>125</sup>I with an active length of 4.2 mm. The Optiseed <sup>103</sup>Pd is composed of two polystyrene cylinders containing active <sup>103</sup>Pd. The active length of <sup>103</sup>Pd is assumed to be 3.8 mm. The <sup>169</sup>Yb and <sup>192</sup>Ir sources have the same geometries with 3.5 mm active core, including radioactive <sup>169</sup>Yb and <sup>192</sup>Ir, respectively. The geometry properties of simulated sources were described in details in the previous published article.<sup>12</sup> The simulations of the sources were verified in that study and the same input files were applied for the mentioned brachytherapy sources in the current study. In that study<sup>12</sup> the verification was based on calculation and comparison of dose rate constant and radial dose function with the corresponding published data on these source models.

## Dosimetric parameters

The updated report of TG-43U1<sup>1</sup> was followed to calculate the dosimetric parameters of low energy brachytherapy sources. For higher energy brachytherapy sources the recommendations by the report of AAPM and ESTRO<sup>2</sup> were applied. Based on the report of TG-43 U1, dose rate is calculated from the following formula:

$$\dot{D}(r, \theta) = S_k \left\langle \frac{G(r, \theta)}{G(r_0, \theta_0)} g(r) F(r, \theta) \right\rangle \quad [1]$$

Geometry function with line-source approximation ( $G_L(r, \theta)$ ), radial dose function ( $g_L(r, \theta)$ ) and two dimensional (2D) anisotropy function ( $F(r, \theta)$ ) are calculated from the following formulas:

$$G_L(r, \theta) = \begin{cases} \frac{\beta}{Lr \sin \theta} & \text{if } \theta \neq 0 \\ \left( r^2 - \frac{L^2}{4} \right)^{-1} & \text{if } \theta = 0 \end{cases} \quad [2]$$

$$g_L(r) = \frac{\dot{D}(r, \theta_0) G(r, \theta_0)}{\dot{D}(r_0, \theta_0) G(r_0, \theta_0)} \quad [3]$$

$$F(r, \theta) = \frac{\dot{D}(r, \theta) G_L(r, \theta_0)}{\dot{D}(r_0, \theta_0) G_L(r_0, \theta)} \quad [4]$$

where  $\beta$  is the angle between the tips of the ends of the active part of source and point of calculation;  $L$  is the active length of the source;  $r$  is the radial distance from the source and the calculation point; and  $\theta$  is the polar angle specifying the calculation point.

### Monte Carlo simulations

MCNPX code (version 2.4.0) was used for the simulations. MCNPX is a general purpose Monte Carlo code and is able to transport neutrons, photons, electrons and other particles in various geometries. It includes a geometry modeling tool and various tallies related to energy deposition, particle current, and particle flux. The 2.4.0 version of this code, which was used in the present study, uses MCPLIB02 cross section library for transport of photons.<sup>13-14</sup> In the MC calculations both photons and electrons were transported. Line-source approximation was used in the MC simulations. The energy cut-off for photons and electrons was considered 1 keV for <sup>125</sup>I and <sup>103</sup>Pd sources and 5 keV for <sup>169</sup>Yb and <sup>192</sup>Ir sources in all input files. No other variance reduction method was applied in this study.

To calculate air kerma strength, air toroid cells were defined in a 100 cm radius vacuum sphere. The brachytherapy source was located at the center of this sphere. The torus cells were in the range of 1–50 cm and their thickness was assumed 1 mm. An F6 tally was scored in these torus cells and the outputs were multiplied by  $r^2$  (where  $r$  is the distance from the center of the source). There are different tallies in MCNP (including F4, \*F4, F6, etc.) which can be utilized to score various dosimetric parameters such as particle flux, energy flux, kerma, etc. In various versions of MCNP code F6 tally is used to score energy deposition averaged over a cell in terms of MeV/g per particle<sup>11</sup>. In other words, kerma is calculated by this tally type. The average of  $F6 \times r^2$  versus  $r$  on the flat region of the curve was calculated to obtain air kerma strength. After obtaining air kerma strength, its value per mCi was calculated for each photon energy spectrum and source. The number of particles transported was  $5 \times 10^7$  and type A statistical uncertainty was less than 1.4% in this step.

To obtain the dose rate constant, an \*F4 tally was calculated at  $r_0 = 1$  cm and  $\theta_0 = \pi/2$ . \*F4 tally is en-

ergy flux of a particle type averaged over a cell (in terms of MeV/cm<sup>2</sup>).<sup>11</sup> It should be noticed that with F4 and \*F4 tallies in MCNP, it is possible to score particle flux and energy flux in a cell, respectively. In other words, the asterisk sign determines that energy flux be scored by the code, and not particle flux. The outputs of this tally were multiplied by mass energy absorption coefficients at various energy bins and the dose was obtained. The dose was divided to air kerma strength value for each source. Additionally, the dose rate at  $r = 1$  cm per mCi for each photon energy spectrum and each source was calculated. Radial dose function was calculated in 1 mm thickness torus cells at radial distances of 0.5–15 cm in a spherical water phantom. The phantom radius was assigned 50 cm and an \*F4 tally was scored and then converted to dose. The number of particle histories for the dose rate constant and radial dose function calculations was  $10^8$  for <sup>125</sup>I, <sup>169</sup>Yb, and <sup>192</sup>Ir and  $3 \times 10^8$  for <sup>103</sup>Pd source. The maximum type A statistical uncertainty was 4.16%.

The 2D anisotropy function was calculated at 0°–180° with a degree interval of 10° at radial distances of 0.5, 1, 5, 10, and 15 cm. The source was located at the center of a spherical water phantom with a 50 cm radius and an \*F4 tally was calculated. Spherical cells were used for 0° and 180° polar angles while torus cells were defined for the other polar angles. The number of particles for this section was assumed as  $2 \times 10^8$  for <sup>169</sup>Yb and <sup>192</sup>Ir sources;  $9 \times 10^8$  for <sup>125</sup>I source; and  $2 \times 10^9$  for <sup>103</sup>Pd source. In all of the data points, the Type A statistical uncertainty was less than 4.18%, with exceptions for two points with 13.8% uncertainty at 0° and 180° angles in 15 cm distance for the <sup>103</sup>Pd source. These uncertainties could not be reduced because it was not possible to exceed the maximum particle history of  $2 \times 10^9$  in MCNP.

To plot isodose curves for a source, a mesh grid was defined in a 50 cm spherical water phantom. The sources were defined in the phantom, separately. For the purpose of output calculation, “pedep” option of type 1 mesh tally type in MCNP was applied in the grid. In MCNP, there are various mesh tallies (including type 1, type 2, type 3, etc.) which can be used to score different dosimetric variables in a grid. Each mesh tally has various options, by which the user defines that which variable should be scored by the code. As an example, type 1 tally is track-average mesh tally. With “pedep” option in this mesh tally type, the average energy deposition per unit volume (in terms of MeV/cm per source particle) for a specified particle type is calculated. This option allows the user to score the equivalent

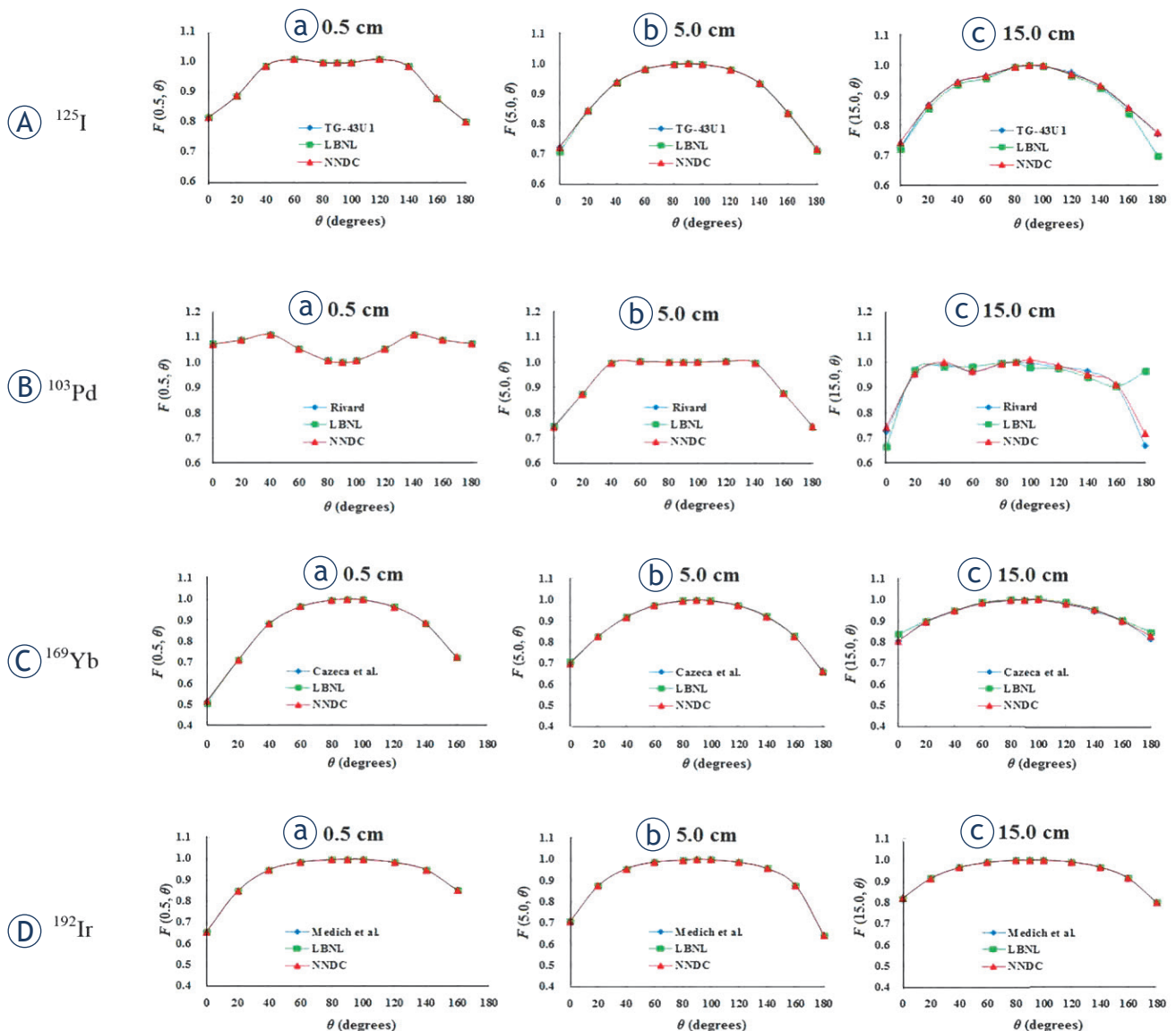


FIGURE 1. 2D anisotropy function values for (A)  $^{125}\text{I}$ , (B)  $^{103}\text{Pd}$ , (C)  $^{169}\text{Yb}$  and (D)  $^{192}\text{Ir}$  sources at  $r = 0.5$  cm (a), 5.0 cm (b), and 15.0 cm (c) distances.

of F6 tally. The grid included  $2 \times 2 \times 2 \text{ mm}^3$  and the obtained data was plotted in the Y-Z plane using MATLAB software (version: 8.3.0.532, The Mathworks, Inc., Natwick, MA).<sup>15</sup> The number of particles for  $^{125}\text{I}$ ,  $^{169}\text{Yb}$ , and  $^{192}\text{Ir}$  sources was  $6 \times 10^8$  photons while it was  $1.5 \times 10^9$  for the  $^{103}\text{Pd}$  source. The type A statistical uncertainty in these mesh voxels was less than 6.5% in the output files.

### The effect of photon energy spectrum

The effect of energy spectrum on dosimetric parameters of  $^{125}\text{I}$ ,  $^{103}\text{Pd}$ ,  $^{169}\text{Yb}$ , and  $^{192}\text{Ir}$  radionuclides was evaluated for three different spectra.

As the first spectrum and via a common method in brachytherapy Monte Carlo studies, the reported photon energy spectra by previous papers were used for the radionuclides.<sup>1,16-18</sup> As the second spectrum database, Lawrence Berkeley National Laboratory (LBNL) was chosen.<sup>19</sup> We applied version 2.1 (January 2004) for all radionuclides in the LBNL database. The third spectrum applied for each radionuclide was extracted from the National Nuclear Data Center (NNDC) database<sup>3</sup> as it was suggested by the report of AAPM and ESTRO.<sup>2</sup> The NNDC database reports a number of energy spectra for a radionuclide. In the present study, these numbers of datasets were chosen from NNDC

**TABLE 1.** Information on photon energy spectra of the  $^{125}\text{I}$  and  $^{103}\text{Pd}$ ,  $^{169}\text{Yb}$ , and  $^{192}\text{Ir}$  radionuclides reported by different databases

	$^{125}\text{I}$			$^{103}\text{Pd}$		
Reference	TG-43 U1 <sup>1</sup>	LBNL <sup>19</sup>	NNDC <sup>20</sup>	Rivard <sup>16</sup>	LBNL <sup>19</sup>	NNDC <sup>21</sup>
Energy range (keV)	27.202-35492	3.335-35.4919	3.77-35.4925	22.074-497.054	2.377-497.08	2.7-487.08
Total photons per disintegration	1.4757	1.60482	1.5767	0.7713825	0.851569801	0.857582605
Average energy (keV)	28.370	27.541	26.059	21.319	19.038	18.889
	$^{169}\text{Yb}$			$^{192}\text{Ir}$		
Reference	Cazeca <i>et al.</i> <sup>17</sup>	LBNL <sup>19</sup>	NNDC <sup>22</sup>	Medich and Munro <sup>18</sup>	LBNL <sup>19</sup>	NNDC <sup>23</sup>
Energy range (keV)	49.77-307.74	6.341-781.64	7.18-781.64	61.49-884.54	7.822-1378.3	9.44-1378.50
Total photons per disintegration	3.322	3.779	3.771	2.301	2.359	2.214
Average energy (keV)	92.797	82.622	82.781	354.356	346.736	369.525

LBNL = Lawrence Berkeley National Laboratory; NNDC = National Nuclear Data Center; TG-43 U1 = Recommendation of the American Association of Physicists in Medicine from task group No. 43 updated report

**TABLE 2.** Air kerma strength, dose rate constant, and dose rate at 1 cm for  $^{125}\text{I}$ ,  $^{103}\text{Pd}$ ,  $^{169}\text{Yb}$ , and  $^{192}\text{Ir}$  sources based on different photon energy spectra reported by other studies, LBNL, and NNDC databases

Source	Other studies <sup>1, 16-18</sup>	LBNL <sup>19</sup>	NNDC <sup>20-23</sup>	Diff. (%) Other study-NNDC	Diff. (%) LBNL-NNDC
$^{125}\text{I}$	1.035	1.169	1.121	-7.67	4.28
$^{103}\text{Pd}$	1.132	1.428	1.404	-19.37	1.71
$^{169}\text{Yb}$	1.094	1.094	1.097	-0.27	-0.27
$^{192}\text{Ir}$	3.622	3.631	3.496	3.60	3.86
Dose rate constant (cGy/hU)					
$^{125}\text{I}$	1.115	0.961	1.013	10.07	-5.13
$^{103}\text{Pd}$	0.830	0.658	0.669	24.06	-1.64
$^{169}\text{Yb}$	1.222	1.226	1.222	0.00	0.33
$^{192}\text{Ir}$	1.117	1.117	1.117	0.00	0.00
Dose rate at 1 cm (cGy/hmCi)					
$^{125}\text{I}$	1.154	1.123	1.136	1.60	-1.07
$^{103}\text{Pd}$	0.939	0.940	0.939	0.00	0.09
$^{169}\text{Yb}$	1.338	1.341	1.341	-0.23	0.00
$^{192}\text{Ir}$	4.045	4.054	3.904	3.59	3.84

LBNL = Lawrence Berkeley National Laboratory; NNDC = National Nuclear Data Center

database: dataset No. 1 for  $^{125}\text{I}$ <sup>20</sup>, dataset No. 1 for  $^{103}\text{Pd}$ <sup>21</sup>, dataset No. 2 for  $^{169}\text{Yb}$ <sup>22</sup> and dataset No. 4 for  $^{192}\text{Ir}$ <sup>23</sup> radionuclides.

The photon energy spectra of  $^{125}\text{I}$ ,  $^{103}\text{Pd}$ ,  $^{169}\text{Yb}$ , and  $^{192}\text{Ir}$  radionuclides reported by various databases are listed in Table 1. The photon energy spectra applied for the  $^{125}\text{I}$  source are: AAPM TG-43 U1 report<sup>1</sup>, LBNL database<sup>19</sup>, and NNDC database<sup>20</sup>. For the  $^{103}\text{Pd}$  source, the photon energy spectra reported by a study by Rivard<sup>16</sup>, LBNL database<sup>19</sup>,

and NNDC database<sup>21</sup> were used. The photon energy spectra applied for the  $^{169}\text{Yb}$  source are: the study by Cazeca *et al.*<sup>17</sup>, LBNL database<sup>20</sup>, and NNDC database<sup>22</sup>. For the  $^{192}\text{Ir}$  source, we extracted the photon energy spectra reported by Medich and Munro<sup>18</sup>, LBNL database<sup>19</sup>, and NNDC database<sup>23</sup>.

In MCNPX code, the photon energy spectrum should be introduced for a source in terms of energies of photons (MeV) emitted by the radionuclide and their intensities. For the four sources, it was

**TABLE 3.** Radial dose function for  $^{125}\text{I}$ ,  $^{103}\text{Pd}$ ,  $^{169}\text{Yb}$ , and  $^{192}\text{Ir}$  sources based on different photon energy spectra reported by other studies<sup>1,16-18</sup>, Lawrence Berkeley National Laboratory (LBNL)<sup>19</sup>, and National Nuclear Data Center (NNDC)<sup>20-23</sup> databases

Source	r (cm)	Other studies (A)	LBNL (B)	NNDC (C)	Diff. (%) A-C	Diff. (%) B-C	Source	Other studies (A)	LBNL (B)	NNDC (C)	Diff. (%) A-C	Diff. (%) B-C
$^{125}\text{I}$	0.5	0.996	0.996	0.996	0.00	0.00	$^{103}\text{Pd}$	1.196	1.196	1.196	0.00	0.00
	1	1.000	1.000	1.000	0.00	0.00		1.000	1.000	1.000	0.00	0.00
	1.5	0.955	0.955	0.954	0.11	0.10		0.789	0.789	0.789	0.00	0.00
	2	0.890	0.890	0.890	0.00	0.00		0.609	0.609	0.608	0.16	0.16
	2.5	0.816	0.815	0.816	0.00	-0.12		0.465	0.465	0.464	0.22	0.22
	3	0.740	0.740	0.740	0.00	0.00		0.352	0.352	0.352	0.00	0.00
	3.5	0.667	0.666	0.667	0.00	-0.15		0.265	0.265	0.264	0.38	0.38
	4	0.596	0.596	0.595	0.17	0.17		0.199	0.199	0.198	0.50	0.51
	4.5	0.530	0.530	0.530	0.00	0.00		0.150	0.150	0.149	0.67	0.68
	5	0.470	0.469	0.470	0.00	-0.21		0.112	0.112	0.112	0.00	0.00
	5.5	0.415	0.415	0.415	0.00	0.00		0.084	0.084	0.083	1.20	1.21
	6	0.365	0.365	0.365	0.00	0.00		0.063	0.062	0.062	1.61	0.00
	6.5	0.320	0.319	0.319	0.31	0.00		0.047	0.047	0.047	0.00	0.00
	7	0.279	0.279	0.279	0.00	0.00		0.035	0.035	0.035	0.00	0.00
	10	0.120	0.120	0.120	0.00	0.00		0.0066	0.0066	0.0065	1.54	1.54
15	0.029	0.029	0.029	0.00	0.00	0.0010	0.0010	0.0010	0.00	0.00		
$^{169}\text{Yb}$	0.5	0.950	0.949	0.951	-0.11	-0.21	$^{192}\text{Ir}$	0.996	0.996	0.996	0.00	0.00
	1	1.000	1.000	1.000	0.00	0.00		1.000	1.000	1.000	0.00	0.00
	1.5	1.042	1.041	1.041	0.10	0.00		1.003	1.003	1.003	0.00	0.00
	2	1.079	1.079	1.077	0.19	0.19		1.006	1.006	1.006	0.00	0.00
	2.5	1.113	1.111	1.110	0.27	0.09		1.008	1.008	1.008	0.00	0.00
	3	1.136	1.137	1.133	0.27	0.35		1.010	1.010	1.009	0.10	0.10
	3.5	1.157	1.156	1.155	0.17	0.09		1.011	1.011	1.010	0.10	0.01
	4	1.169	1.171	1.168	0.09	0.26		1.011	1.011	1.010	0.10	0.10
	4.5	1.183	1.181	1.180	0.25	0.09		1.010	1.010	1.010	0.00	0.00
	5	1.189	1.185	1.185	0.34	0.00		1.008	1.008	1.007	0.10	0.10
	5.5	1.193	1.191	1.191	0.17	0.00		1.005	1.005	1.005	0.00	0.00
	6	1.195	1.189	1.190	0.42	-0.08		1.002	1.002	1.001	0.10	0.10
	6.5	1.189	1.185	1.186	0.25	-0.08		0.998	0.998	0.998	0.00	0.00
	7	1.182	1.181	1.181	0.09	0.00		0.995	0.994	0.994	0.10	0.00
	10	1.089	1.091	1.090	-0.09	0.09		0.949	0.949	0.949	0.00	0.00
15	0.860	0.865	0.862	-0.23	0.35	0.836	0.836	0.835	0.12	0.12		

not feasible to list all the energies and the related probabilities in a single table or figure. Therefore, some information including the energy range, total intensity, and average energy are listed in Table 1.

TG-43 parameters were calculated for  $^{125}\text{I}$ ,  $^{103}\text{Pd}$ ,  $^{169}\text{Yb}$ , and  $^{192}\text{Ir}$  sources with three specific photon energy spectra to evaluate whether the photon energy spectrum effect the dosimetric parameters.



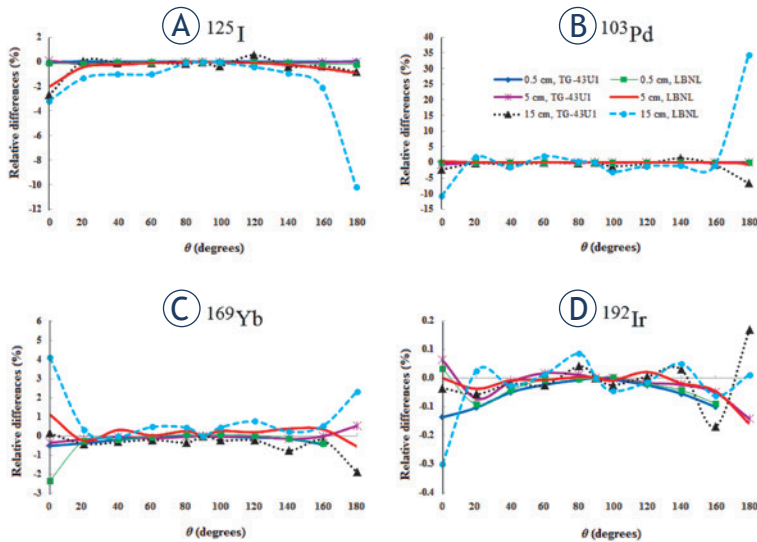


**FIGURE 2.** Percentage differences (%) between the 2D anisotropy function obtained from National Nuclear Data Center (NNDC) and other references of energy spectra for (A)  $^{125}\text{I}$ , (B)  $^{103}\text{Pd}$ , (C)  $^{169}\text{Yb}$ , and (D)  $^{192}\text{Ir}$  sources.

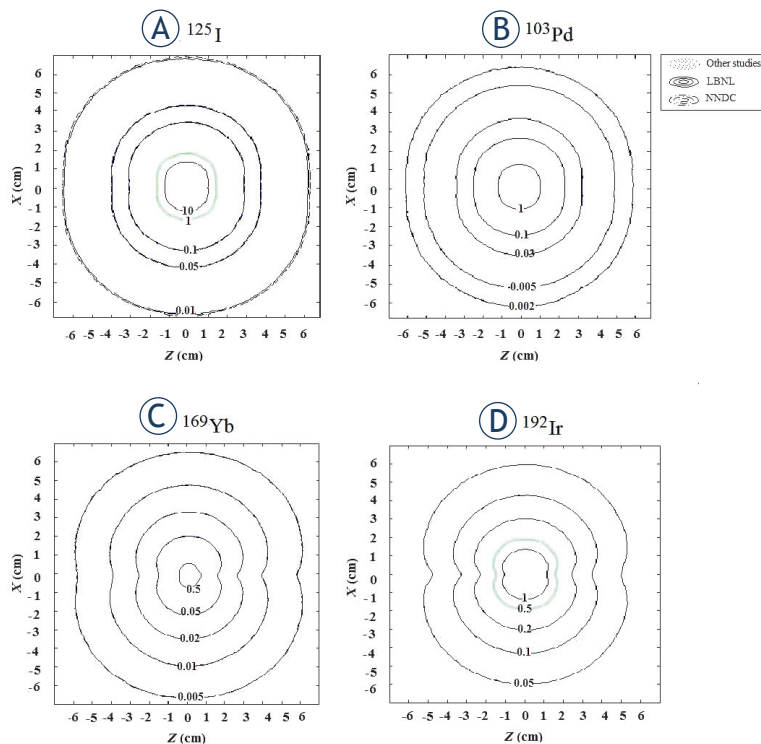


**FIGURE 3.** Isodose curves for (A)  $^{125}\text{I}$ , (B)  $^{103}\text{Pd}$ , (C)  $^{169}\text{Yb}$ , and (D)  $^{192}\text{Ir}$  sources obtained by different photon energy spectra. The contours for various spectra are not clearly distinguishable due to their overlapping.

## Results

The values of air kerma strength per activity were calculated for MED 3631-A/M  $^{125}\text{I}$ , Optiseed  $^{103}\text{Pd}$ , a hypothetical  $^{169}\text{Yb}$ , and Flexisource  $^{192}\text{Ir}$  sources. These values are presented in Table 2 for three

photon energy spectra for each of these sources. Furthermore, dose rate constant and dose rate at  $r = 1$  cm are presented in Table 2. The values of radial dose function at  $r = 0.5$ – $15$  cm with the three photon energy spectra for  $^{125}\text{I}$ ,  $^{103}\text{Pd}$ ,  $^{169}\text{Yb}$ , and  $^{192}\text{Ir}$  sources are listed in Table 3.

2D anisotropy function calculated at  $\theta = 0^\circ$ – $180^\circ$  angles for  $r = 0.5$ ,  $5$ , and  $15$  cm distances for  $^{125}\text{I}$ ,  $^{103}\text{Pd}$ ,  $^{169}\text{Yb}$ , and  $^{192}\text{Ir}$  sources are illustrated in Figure 1. The differences between the anisotropy function data based on NNDC photon energy spectrum and the other spectra are shown in Figure 2. The isodose curves for  $^{125}\text{I}$ ,  $^{103}\text{Pd}$ ,  $^{169}\text{Yb}$ , and  $^{192}\text{Ir}$  sources based on different energy spectra reported by articles<sup>1,16–18</sup>, LBNL<sup>19</sup> and NNDC<sup>20–23</sup> are contoured in Figure 3. In this figure the dose values are related to the values in the Z-X plane while the source's longitudinal axis is along the Z-axis. The dose values are normalized to the dose at  $r = 1$  cm for each source.

## Discussion

In the current study, the influence of photon energy spectrum on dosimetric parameters of  $^{125}\text{I}$ ,  $^{103}\text{Pd}$ ,  $^{169}\text{Yb}$ , and  $^{192}\text{Ir}$  brachytherapy sources was evaluated. Dose rate constant is the ratio of dose rate at 1 cm to air kerma strength. All these quantities are presented in Table 2 for the considered sources. The relative difference values of dose rate constant with regard to NNDC based data, shows a maximum value of 24.06% and 10.07% for the  $^{103}\text{Pd}$  and  $^{125}\text{I}$  brachytherapy sources, respectively (Table 2). These percentage differences are related to the photon energy spectra by TG-43 U1 protocol<sup>1</sup> and NNDC<sup>20</sup> database for the  $^{125}\text{I}$  source; and LBNL<sup>19</sup> and NNDC database<sup>21</sup> for the  $^{103}\text{Pd}$  source. There are non-negligible differences between the dose rate constant values obtained by different photon energy spectra databases for the  $^{125}\text{I}$  and  $^{103}\text{Pd}$  sources. Table 2 demonstrates that the cause of these differences is due to air kerma strengths. The effect for air kerma strength to the differences in total number of photons per disintegration (Table 1) and the differences in photon energy in various spectra demonstrate their main cause is air kerma strength. In other words, for calculation of air kerma strength the environment is void and minor differences in photon energy have a major effect on the kerma rate. This effect is not seen for dose rate at 1 cm in which the media is water.

The radial dose function calculated by different photon energy spectra does not show a consider-

able difference between brachytherapy sources. The differences do not show a general trend with distance. The minor effect of energy spectrum on radial dose function is in agreement with the results by Rivard *et al.*<sup>8</sup> In that study, the effect of energy spectrum on dose rate constant and radial dose function ranged from 0.1% to 2%. The values of anisotropy function illustrated in Figure 1 show a similar trend for all applied photon energy spectra of brachytherapy sources. As illustrated in Figure 2, there are some points that a non-negligible difference is observable. This figure refers a larger difference at  $\theta = 0^\circ$  and  $180^\circ$  at far distances from the  $^{103}\text{Pd}$ ,  $^{125}\text{I}$  and  $^{169}\text{Yb}$  sources, respectively. Furthermore, as it can be seen from the range of vertical axis of Figure 2, the difference of anisotropy function values with regard to the values calculated by NNDC spectra databases,  $^{103}\text{Pd}$ ,  $^{125}\text{I}$ , and  $^{169}\text{Yb}$  show the maximum differences. For the  $^{103}\text{Pd}$  source, about 35% difference was observed between anisotropy function calculated based on the photon energy spectra reported by LBNL and NNDC databases. The reason for the differences in the  $0^\circ$  and  $180^\circ$  degrees for  $^{103}\text{Pd}$  is related to the uncertainty in the Monte Carlo calculations (13.8%), therefore they may be independent of the effect of photon spectrum. In the current study no variance reduction method was applied except for energy cut offs. For future studies, it is suggested to apply such methods to reduce the statistical uncertainties, especially for the  $^{103}\text{Pd}$  source.

As it is seen in Figure 3, there is no observable difference in isodose curves of  $^{125}\text{I}$ ,  $^{103}\text{Pd}$ ,  $^{169}\text{Yb}$ , and  $^{192}\text{Ir}$  sources with different photon energy spectra. However, this doesn't mean that the photon energy spectrum choice for a radionuclide doesn't affect dose distribution around the source. As it was implied from the obtained data of TG-43 dosimetric parameters, such as air kerma strength and dose rate constant values, this effect is not negligible. On the other hand, isodose contours cannot show such differences. Relying only on isodose curves for clinical application of brachytherapy sources may induce some errors in quantification of dose values.

For different photon energy spectra the calculated mean energies were in relatively good agreement for both LBNL and NNDC databases. A maximum of 24.06% difference was observed between dose rate constant of different energy databases. Ignoring the differences in the anisotropy function values at  $\theta = 0^\circ$  and  $180^\circ$  degrees, especially for the  $^{103}\text{Pd}$  source which originate from the Monte Carlo calculation uncertainties, there are minor differences in dosimetric parameters of the

studied sources for various energy spectrum references. Additionally no considerable difference was observed in isodose curves of different photon energy spectra. Generally it can be concluded that while these differences are not considerable, due the fact that the total uncertainty in dose delivery in radiotherapy should not exceed  $\pm 5\%$  (ICRU report No. 24<sup>24</sup>), it is recommended that more accurate and updated photon energy spectrum databases be used in Monte Carlo simulation and other radiotherapy applications of brachytherapy sources. This is to minimize the related uncertainties in clinical applications of the sources and is in accordance with the AAPM and ESTRO guideline on simulation of brachytherapy sources.<sup>2</sup>

## Acknowledgment

The authors would like to thank Sabzevar University of Medical Sciences for financial support of this work.

## References

- Rivard MJ, Coursey BM, DeWerd LA, Hanson WF, Huq MS, Ibbott GS, et al. Update of AAPM task group No. 43 report: a revised AAPM protocol for brachytherapy dose calculations. *Med Phys* 2004; **31**: 633-74.
- Perez-Calatayud J, Ballester F, Das RK, Dewerd LA, Ibbott GS, Meigooni AS, et al. Dose calculation for photon-emitting brachytherapy sources with average energy higher than 50 keV: Report of the AAPM and ESTRO. *Med Phys* 2012; **39**: 2904-29.
- National Nuclear Data Center (NNDC); 2007, Available at: <http://www.nndc.bnl.gov>. [Accessed 22 Jan 2016].
- Keillor ME, Aalseth CE, Day AR, Fast JE, Hoppe EW, Hyronimus BJ, et al. Design and construction of an ultra-low-background 14-crystal germanium array for high efficiency and coincidence measurements. *J Radioanal Nucl Chem* 2009; **282**: 703-8.
- Nedera H, Heussera G, Laubensteinb M. Low level  $\gamma$ -ray germanium-spectrometer to measure very low primordial radionuclide concentrations. *Appl Radiat Isotopes* 2000; **53**: 191-5.
- Karamanis D. Efficiency simulation of HPGe and Si (Li) detectors in  $\gamma$ - and X-ray spectroscopy. *Nucl Instr Meth Phys Res* 2003; **505**: 282-5.
- Chen Z, Bongiorno P, Nath R. Experimental characterization of the dosimetric properties of a newly designed I-Seed model AgX100  $^{125}\text{I}$  interstitial brachytherapy source. *Brachytherapy* 2012; **11**: 476-82.
- Rivard MJ, Granero D, Perez-Calatayud J, Ballester F. Influence of photon energy spectra from brachytherapy sources on Monte Carlo simulations of kerma and dose rates in water and air. *Med Phys* 2010; **37**: 869-76.
- Aryal P, Molloy JA, Rivard MJ. A modern Monte Carlo investigation of the TG-43 dosimetry parameters for an  $^{125}\text{I}$  seed already having AAPM consensus data. *Med Phys* 2014; **41**: 021702.
- Luse RW, Blasko J, Grimm P. A method for implementing the American Association of Physicists in Medicine Task Group-43 dosimetry recommendations for  $^{125}\text{I}$  transperineal prostate seed implants on commercial treatment planning systems. *Int J Radiat Oncol Biol Phys* 1997; **37**: 737-41.
- Waters LS. *MCNPX user's manual*. Version 2.4.0. Report LA-CP-02-408 (Los Alamos, New Mexico: Los Alamos National Laboratory; 2000.



12. Moghaddas TA, Ghorbani M, Haghparast A, Flynn RT, Eivazi MT. A Monte Carlo study on dose enhancement effect of various paramagnetic nanoshells in brachytherapy. *J Med Biol Eng* 2014; **34**: 559-67.
13. Gifford KA, Mourtada F, Cho SH, Lawyer A, Horton JL Jr. Monte Carlo calculations of the dose distribution around a commercial gynecologic tandem applicator. *Radiother Oncol* 2005; **77**: 210-5.
14. Bahreyni Toossi MT, Abdollahi M, Ghorbani M. A Monte Carlo study on dose distribution validation of GZP6 <sup>60</sup>Co stepping source. *Rep Pract Oncol Radiother* 2013; **18**: 112-6.
15. MathWorks Inc., Available at: <http://www.mathworks.com/matlabcentral/>. [Accessed 22 Jan 2016].
16. Rivard MJ. A discretized approach to determining TG-43 brachytherapy dosimetry parameters: case study using Monte Carlo calculations for the MED3633 <sup>103</sup>Pd source. *Appl Radiat Isotopes* 2001; **55**: 775-82.
17. Cazeca MJ, Medich DC, Munro JJ 3rd. Monte Carlo characterization of a new Yb-169 high dose rate source for brachytherapy application. *Med Phys* 2010; **37**: 1129-36.
18. Medich DC, Munro JJ 3rd. Monte Carlo characterization of the M-19 high dose rate Iridium-192 brachytherapy source. *Med Phys* 2007; **34**: 1999-2006.
19. LBNL Isotopes Project - LUNDS Universitet. Available at: <http://ie.lbl.gov/toi/index.asp>. [Accessed 22 Jan 2016].
20. National Nuclear Data Center (NNDC); 2007. Available at: <http://www.nndc.bnl.gov/chart/decaysearchdirect.jsp?nuc=125I&unc=nds>. [Accessed 22 Jan 2016].
21. National Nuclear Data Center (NNDC); 2007. Available at: <http://www.nndc.bnl.gov/chart/decaysearchdirect.jsp?nuc=103PD&unc=nds>. [Accessed 22 Jan 2016].
22. National Nuclear Data Center (NNDC); 2007, Available at (<http://www.nndc.bnl.gov/chart/decaysearchdirect.jsp?nuc=169YB&unc=nds>), [accessed at 22 January 2016].
23. National Nuclear Data Center (NNDC); 2007. Available at: <http://www.nndc.bnl.gov/chart/decaysearchdirect.jsp?nuc=192IR&unc=nds>. [Accessed 22 Jan 2016].
24. International Commission on Radiation Units and Measurements. *Determination of absorbed dose in a patient irradiated by beams of X or gamma rays in radiotherapy procedures*. Washington, Bethesda: ICRU; 1976. Report No: ICRU-24.